River Flow 2010 - Dittrich, Koll, Aberle & Geisenhainer (eds) - © 2010 Bundesanstalt für Wasserbau ISBN 978-3-939230-00-7

Velocity profiles in dam-break flows: Water and sediment layers

R. Aleixo
Department of Civil and Environmental Engineering, Université catholique de Louvain. B-1348 Louvain-la-Neuve, Belgium

S. Soares-Frazão & B. Spinewine
Fonds de la Recherche Scientifique-FNRS and Department of Civil and Environmental Engineering, Université catholique de Louvain, B-1348 Louvain-la-Neuve, Belgium

Y. Zech
Department of Civil and Environmental Engineering, Université catholique de Louvain. B-1348 Louvain-la-Neuve, Belgium

ABSTRACT: To gain a deeper understanding of the physics of a dam-break flow, detailed measurements that go beyond measurements of macro-scale variables such as water-depth evolution and water-front celerity are needed. These measurements should focus on the determination of the velocity profiles and on the description of flow-bed interactions. A dam-break propagating over a loose sediment bed will induce sediment transport and in this process two moving layers can be distinguished, namely a clear-water layer and a sediment-laden layer. A deeper understanding of dam-break flows is therefore directly connected to the behaviour and the mutual interactions of those two layers. Such a two-layer description may be used in numerical modelling, for which some assumptions are commonly made, e.g., a simplified uniform velocity profile in each of the moving layers. Improvements in image acquisition techniques have made it possible to measure the actual velocities in the two layers. In this paper a study of the velocity profiles in a dam break flow, both for water layer and sediment layer, is presented. The measurements were made by means of a Particle Image Velocimetry (PIV) system. They allow the determination of the velocity field in the water and sediment layers, giving some insight about the interactions between those two layers.

Keywords: Dam-break flow, Experiments, PIV, Sediment

1 INTRODUCTION

The study of dam-break flows is a challenge whatever the approach: experimental, numerical, and theoretical. In the particular case of experimental research adequate techniques are needed to capture the essential features of the flow. In the past the experimental analysis of a dam-break flow mainly focused on macroscopic variables of the problem, e.g. water height evolution and wave celerity (Lauber & Hager, 1998). The transient nature of a dam break flow inhibits the application of intrusive techniques and/or point-wise techniques such Laser Doppler Velocimetry (LDV), but opens the way to the application of image-based techniques such as Particle Image Velocimetry (PIV) and Particle Tracking Velocimetry (PTV).

In this study, PIV measurements were carried out on a dam break flow over loose sediment bed and the velocity fields of the water and sediment layers were simultaneously determined.

1.1 *Dam break flows generalities*

Dam-break flows are transient flows that have been studied since the end of the XIXth century (Stoker, 1957). These flows may be considered either over fixed bed, hereafter designated as hydrodynamic case, or over a moving sediment layer, referred in this paper as sedimentologic case. The scaling variables for this kind of flow are the initial water height, h_0 and the gravity's acceleration, g. With these two variables it is possible to define a velocity scale, c_0, and a time scale, T_0, given respectively by (Stoker, 1957):

$$c_0 = \sqrt{g h_0} \tag{1}$$

$$T_0 = \sqrt{\frac{h_0}{g}} \tag{2}$$

Non-dimensional horizontal and vertical velocity components are then obtained respectively as

$$U = \frac{u}{c_0} \quad \text{and} \quad W = \frac{w}{c_0} \tag{3}$$

Non-dimensional horizontal and vertical coordinates and time are scaled respectively as

$$X = \frac{x}{h_0}, \qquad Z = \frac{z}{h_0} \quad \text{and} \quad T = \frac{t}{T_0} \tag{5}$$

The gate is considered to be at $X = 0$. For the sedimentologic dam break flow, i.e. over a bed of loose sediments, one has to take into account not only the water-layer velocity field but also the velocity of the moving sediment layer. A possible simplified model is schematized in Figure 1, where uniform velocity is assumed both in the clear-water layer as in the sediment layer (e.g. Spinewine, 2005 and Zech et al. 2008).

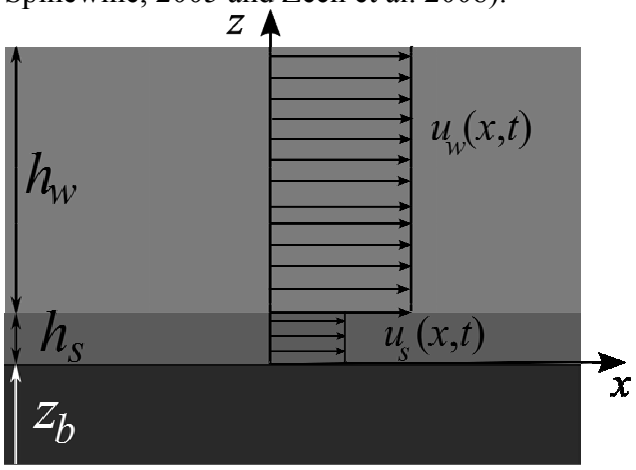

Figure 1 Sketch of a two layer model. The different layers are h_w the water layer, h_s the moving sediment layer and z_b the fixed bed level. The velocity profiles for the water and sediment layers are denoted by u_w and u_s, respectively.

Some previous works have shed some light on the velocity profiles of each layer separately. According to Van Goethem & Villers (2000), the sediment layer follows a linear velocity profile, whereas, according to Aleixo et al. (2009) following an analysis made by Voisin & Greindl (2007) the velocity profile of the water layer is practically uniform in the near-field of the dam-break flow, i.e. in the first instants after gate opening, and close to the gate.

2 PARTICLE IMAGE VELOCIMETRY

Particle Image Velocimetry is nowadays an established and mature measurement technique (Raffel et al., 2007). It allows measuring the instantaneous velocity field based on the cross-correlation of two flow images obtained over a short time period Δt.

Let one consider a double-pulsed laser, which by means of an appropriated diverging optics, produces a light sheet illuminating a section of a flow previously seeded with particles, as depicted in Figure 2. Consider also a camera that is synchronized with the laser, acquiring one image for each of the two laser pulses. The consecutive images are then separated in smaller areas designated as interrogation windows. The interrogation windows of the first image I1 are correlated with the corresponding interrogation windows of the second image I2 (Keane and Adrian, 1992) as depicted in Figure 2. The displacement of the correlation peak will be a measurement of the most probable displacement of the particle's ensemble of each interrogation window. So, having the displacement vector and knowing the time interval between laser pulses, the velocity vector for each interrogation window, *i*, is obtained as:

$$\mathbf{v}_i = \frac{\mathbf{x}_i}{dt} \tag{6}$$

where $\mathbf{v}_i$ is the velocity vector of interrogation window *i*, $\mathbf{x}_i$ is the displacement vector of the correlation peak and *dt* is the time interval between pulses.

Using one camera for the image acquisition, PIV allows the determination of two of the components of the velocity vector in the light sheet plane.

In modern PIV algorithms the detection of the correlation peak is made with sub-pixel accuracy by fitting a Gaussian curve to the correlation intensity distribution (Raffel et al., 2007). According to the same authors this process leads to accuracies of the order of 0.1 pixel in the determination of displacement vectors. On other hand, the generalization of digital image acquisition has allowed the introduction and use of advanced digital interrogation techniques like multiple-pass interrogation and iterative window deformation, in order to adapt the interrogation windows to flow gradients (Raffel et al. 2007).

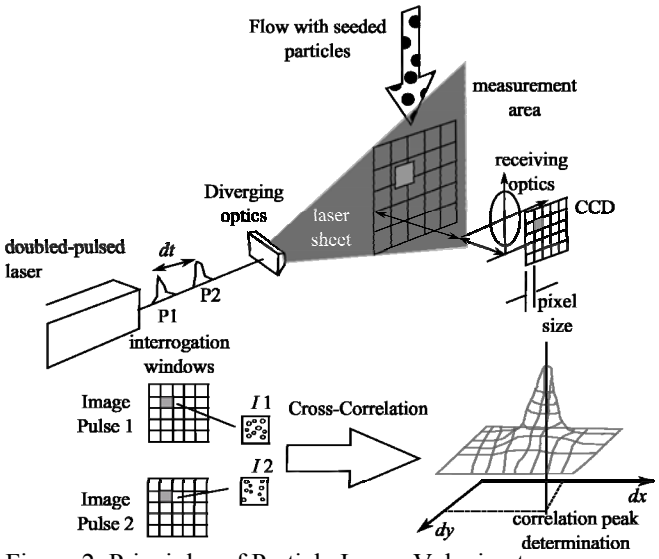

Figure 2. Principles of Particle Image Velocimetry.

3 EXPERIMENTAL SET UP

3.1 *The Dam-Break Channel*

Experiments were conducted in the dam-break channel of the Hydraulics Laboratory at the Université catholique de Louvain, Belgium. It is a constant width rectangular channel with a length of 6 m, a width of 0.25 m and a height of 0.5 m. The channel is divided in two reaches of equal length by a narrow gate controlled by a downward-moving pneumatic jack that allows an opening time of about 120 ms. The reach upstream of the gate is used as a reservoir and the reach downstream is used as test section. The experimental setup is depicted in Figure 3. A detailed description of the facility can be found in Spinewine & Zech (2007) and Bailly & Van Reybroeck (2003).

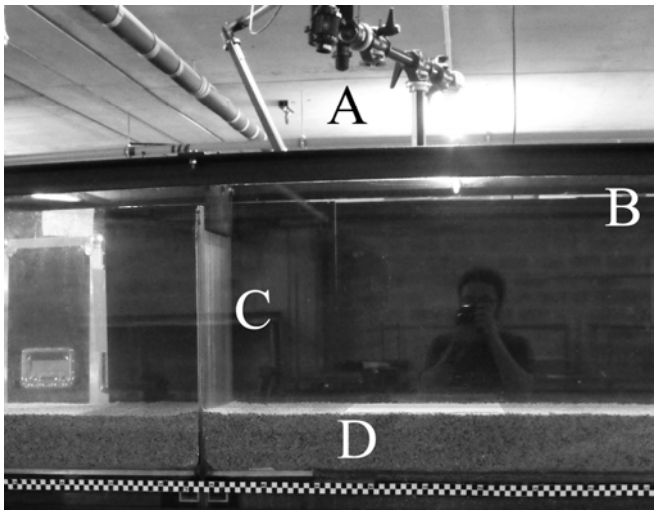

Figure 3. Dam break channel used for the experiments and part of the PIV system. A) Laser light guiding arm and diverging optics to create the light sheet. B) channel structure. C) downward moving gate. D) Sediment bed.

On the channel bed a layer of sand was emplaced, with a thickness of 0.10 m, a density $\rho_s = 2.63\times10^3$ kg.m^{-3} and a $d_{50} = 1.72\times10^{-3}$ m. For each experiment the bed was levelled, compacted and saturated with water in order to ensure the same conditions from one experiment to another. The initial water level in the reservoir was set to 0.325 m for all the three runs. In Table 1 the relevant values are summarized.

According to Lauber & Hager (1998) a dam break can be considered as instantaneous if the gate removal time T_r obeys the relation $T_r < (2h_0/g)^{0.5}$. For $h_0 = 0.325$ m the measured falling time was $T_r = 0.12$ s < 0.25 s. Therefore the dam break can be considered as instantaneous.

Table 1. Experimental conditions

Variable	Value
Channel	
width	0.25 m
height	0.50 m
length	6 m
Sediment	
layer height, h_s	0.10 m
d_{50}	1.72×10^{-3} m
ρ_s	2.63×10^3 kg.m^3
Initial water level h_0	0.325 m

3.2 *The PIV System*

The velocity profiles were measured by means of a LaVision® Particle Image Velocimetry system. This system consists of a double pulsed laser of 30 mJ that is used to light the desired flow region, and a CCD camera of 1.92 Mpix synchronized with the pulsed laser by means of a computer controlled time unit.

The laser beam is guided by an optical arm until reaching the diverging optics system that will transform the laser beam into a laser light sheet. The obtained laser sheet is then positioned parallel to the principal direction of the flow allowing measurements of the two flow components in the vertical and horizontal directions. In Figure 3 it is possible to see the laser light guiding arm (A) on top of the channel.

The main hardware characteristics of the PIV system are listed in Table 2.

Table 2. PIV hardware parameters

Parameter	Value
Lens focal distance and aperture	60 mm / f1.7
Time interval between pulses	1.0 ms < dt < 1.5 ms
Nominal acquisition frequency	15 Hz

Seeding of the flow was made with pliolite particles. In order to break the surface tension the pliolite particles were first immersed in a bath of soapy water and afterwards added to the upstream reservoir.

For the PIV processing a multi-step procedure was used, starting with interrogation windows of 256 × 256 pixels and ending at 32 × 32 pixels. A window overlap of 75% was also considered. This allowed a spatial resolution of about 2 mm.

3.2.1 *PIV Calibration Procedure*

In order to convert pixel units into physical units a calibration must be performed. The latter must be performed in the same imaging conditions as the experiment, i.e. under water. As the test section is not filled with water before the initiation of the experiment, the calibration is performed by placing a calibration target inside the upstream reser-

voir at the desired longitudinal section. For the present case the calibration and measurements were carried out at the centreline of the channel. This calibration target consists in a plate where a matrix of calibration points, equally spaced, are drawn. After filling the reservoir with water the calibration target is immersed and a picture is taken. Through the reference points of the obtained image a 3rd order polynomial is fitted and used as calibration function. This is made automatically by a sub-routine included in the PIV software. The camera and laser are then rigidly translated to the test section downstream the gate, keeping the same imaging configuration.

4 EXPERIMENTAL RESULTS

The time amount needed to prepare one dam-break experience limited the number of tests made. Three independent runs were made and the presented results refer to each one of those runs. A lack of a synchronization signal between the gate and the PIV prevented the possibility of averaging the results of each run. Nevertheless each run allowed to capture the dam-break flow at different time steps and since the dam-break flow has proven to be quite repeatable (Soares-Frazão & Zech, 2008) this procedure allowed to obtain a better temporal resolution than the one provided by the PIV system ($\Delta T = 0.37$ which corresponds to the 15 Hz acquisition rate presented in Table 2)

4.1 *Near Field Measurements – Water Layer*

For the near-field study, three instants were considered, $T = 0.44$, 0.67 and 0.77. These instants were obtained from three different runs and since the dam-break flow shows a good repeatability (Soares-Frazão & Zech, 2008) they are used here to describe the near field. Figure 4 shows the PIV image at $T = 0.44$ and Figure 5 gives the measured velocities at the same instant ($T = 0.44$). It is possible to see on Figure 4 the breaking wave. As the gate is pulled down to simulate the dam break, the falling down movement of the top of the water column might be faster than the horizontal water motion. This will mostly depend on the initial water level and the friction between sediment layer and water layer, and the water solicitation over the sediments. The bed sediments in motion are also captured by the camera, and this will be used later to determine the sediment layer velocity. The velocity-vector fields for the remaining instants are depicted in Figures 6 and 7.

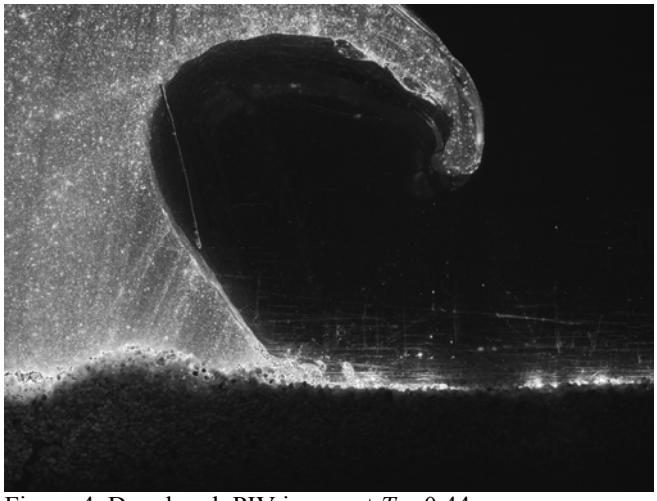

Figure 4. Dam break PIV image at $T = 0.44$.

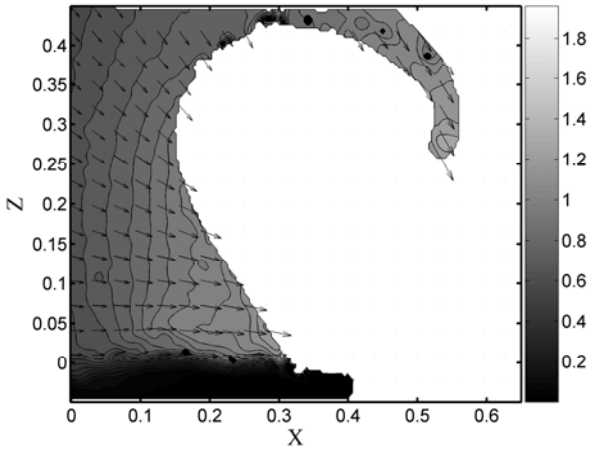

Figure 5. Dam break velocity field for $T = 0.44$. For clarity only 1 out of 8 vectors represented.

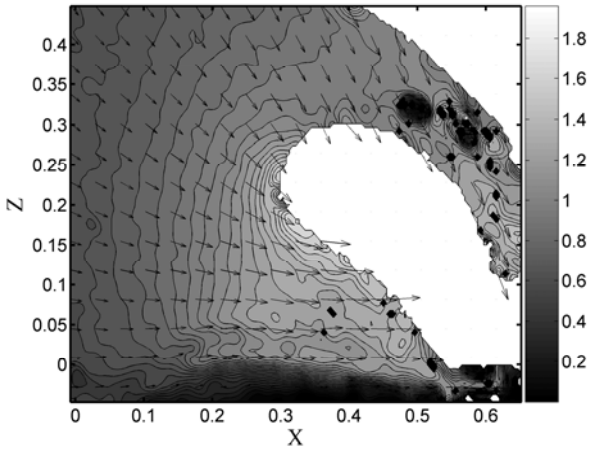

Figure 6. Dam break velocity field for $T = 0.67$. For clarity only 1 out of 8 vectors represented.

For the considered instants $T = 0.44$, 0.67 and 0.77 the velocity profiles for the horizontal and vertical components at $X = 0$ (gate section) are depicted in Figures 8 and 9 respectively. After the acceleration of the flow, there is a deceleration between $T = 0.67$ and $T = 0.77$. For $X = 0$, the flow accelerates more near the bed than near the surface.

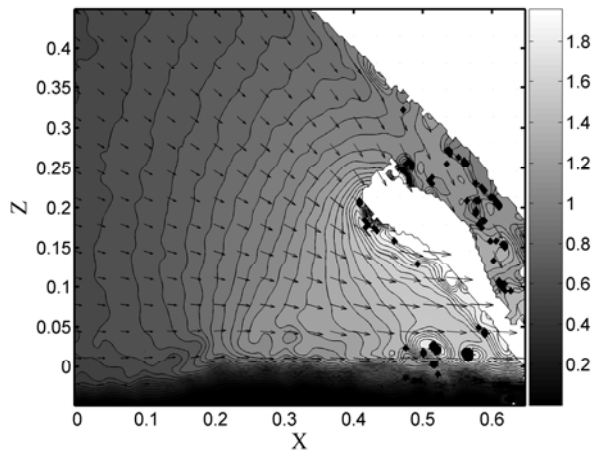

Figure 7. Dam break velocity field for $T = 0.77$. For clarity only 1 out of 8 vectors are represented.

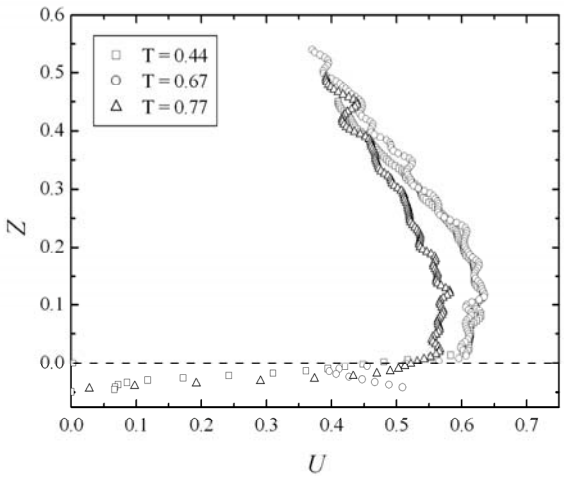

Figure 8. Profiles of horizontal velocity at $X = 0$ (gate section) for $T = 0.44$, 0.67 and 0.77. The dashed line indicates the initial bed level.

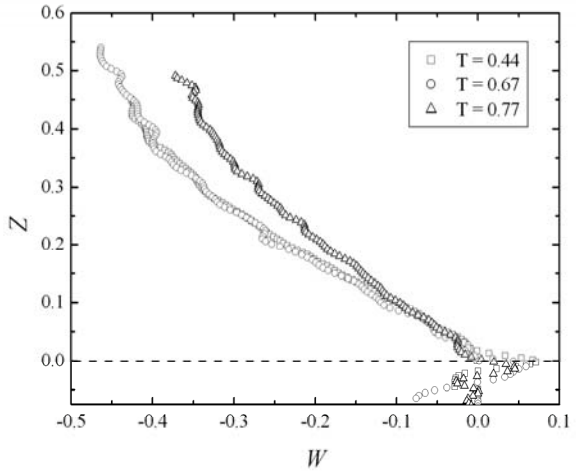

Figure 9. Profiles of vertical velocity at $X = 0$ (gate section) for $T = 0.44$, 0.67 and 0.77. The dashed line indicates the initial bed level.

One of the characteristics associated with the near-field regime of the dam-break flow is the fact that the velocity field has a strong non-horizontal component. This can be seen by drawing in polar coordinates the velocity field modulus and angle as shown in Figure 10, for $T = 0.439$. The most part of the points lie within the 4th quadrant. The points in the 1st quadrant are due to the upward sediment velocity as can be seen Figure 9.

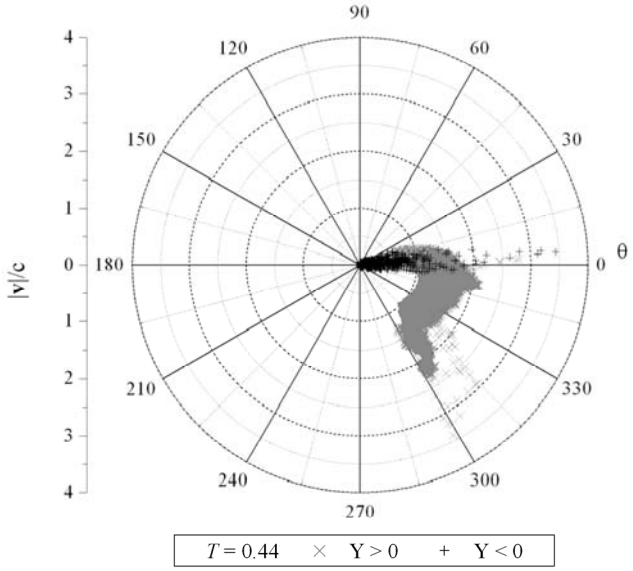

Figure 10. Velocity vector angle and modulus distribution for $T = 0.44$. Concentric circles represent a value of constant velocity norm, whose scale is represented by the vertical line adjacent to the plot.

4.1.1 *Detailed Analysis of the Sediment Layer*

As observed in Figure 4 the moving water will interact with the bed causing it to erode. The motion of sediment particles is captured by the PIV camera and processed with the PIV algorithm just as for the pliolite tracers. Nevertheless one must be careful when processing the results. As it can be seen on Figure 4, not only the sediments present in the laser light sheet plan are visible but also sediments between that plane and the channel sidewall. So the velocity calculation may be biased by this effect.

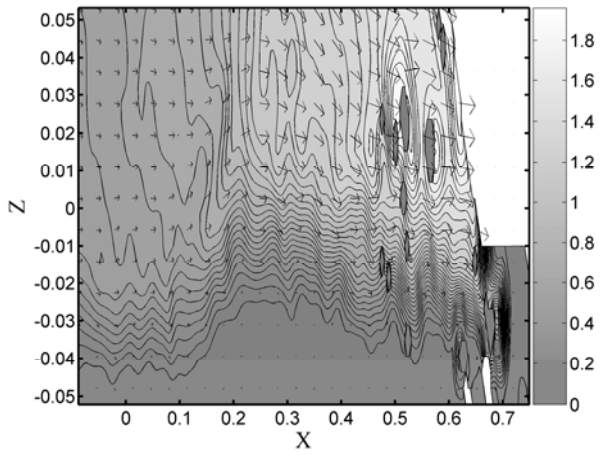

Figure 11. Detail for the velocity field near bed region for $T = 0.439$. For clarity only 1 out of 8 vectors are represented along the horizontal and 1 out of 2 vectors are represented along the vertical.

Contrary to what happens in the water layer, the sediment layer shows a velocity field that has no significant downward component.

4.2 *Far Field Measurements – Water Layer*

As time goes by the dam-break flow is continuously evolving, and the flow characteristics change accordingly. This is quite noticeable on the flow field behaviour when comparing Figure 4 and Figure 12. In Figures 13 to 15 the velocity fields obtained for $T = 4.90$, 5.13 and 5.21 are shown.

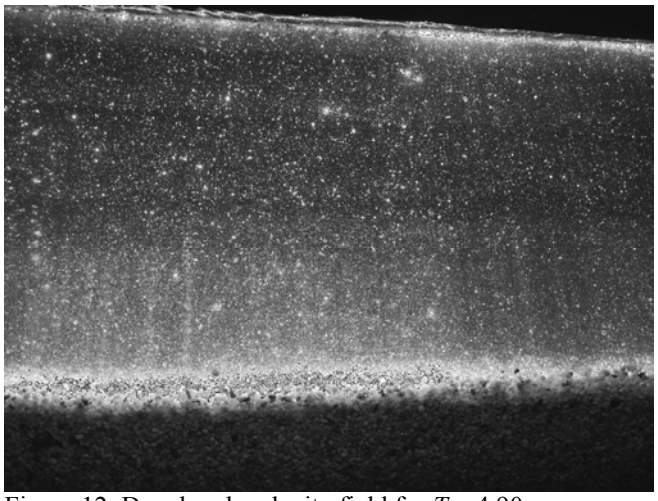

Figure 12. Dam break velocity field for $T = 4.90$.

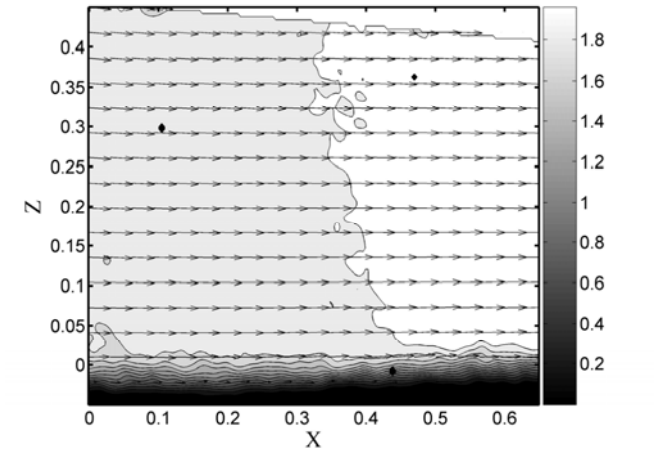

Figure 13. Dam break velocity field for $T = 4.90$. For clarity only 1 out of 8 vectors represented.

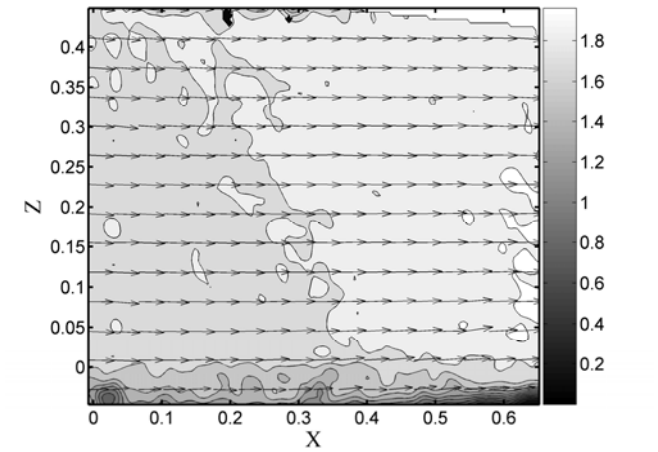

Figure 14. Dam break velocity field for $T = 5.13$. For clarity only 1 out of 8 vectors is represented.

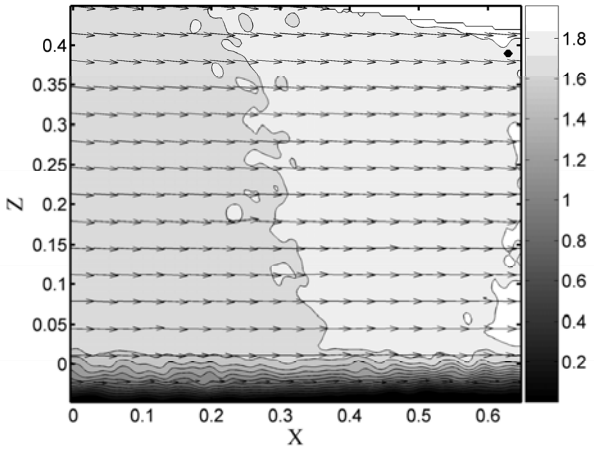

Figure 15. Dam break velocity field for $T = 5.21$. For clarity only 1 out of 8 vectors is represented.

The velocity profiles obtained at $X = 0$ are shown in Figure 16. For the far field the water layer has an approximate constant velocity while the sediment layer still has a linear velocity profile. On the other hand the flow accelerated between the first instants (Figure 8 and 9) and later times (Figure 16 and 17). The velocity increased from about $U \approx 0.55$ at $T = 0.77$ to $U \approx 0.65$ at $T = 5.21$. Also to note is the expected reduction in the flow level, decreasing from $Z \approx 0.55$ at $T = 0.77$ to $Z \approx 0.47$ at $T = 5.21$.

The velocity at $X = 0.5$ is plotted in Figure 18 and 19. It is clear that at $X = 0.5$ there is a slight acceleration of the flow in part caused by the decrease of the water level.

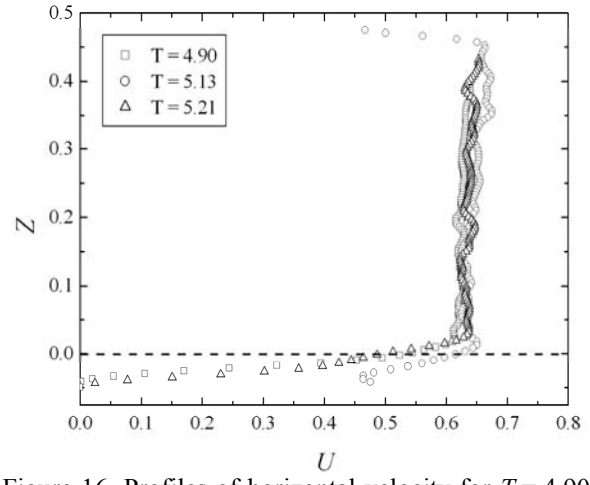

Figure 16. Profiles of horizontal velocity for $T = 4.90$, 5.13 and 5.21 at $X = 0$.

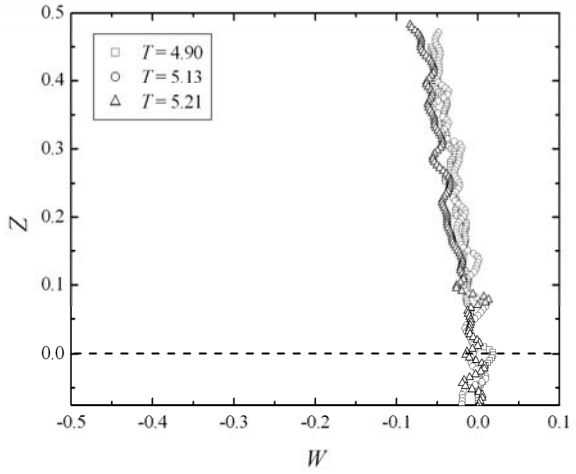

Figure 17. Profiles of vertical velocity for $T = 4.90$, 5.13 and 5.21 at $X = 0$.

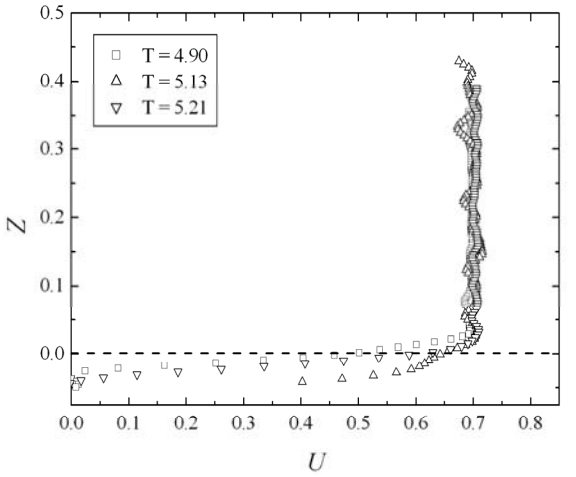

Figure 18. Profiles of horizontal velocity for $T = 4.90$, 5.13 and 5.21 at $X = 0.5$.

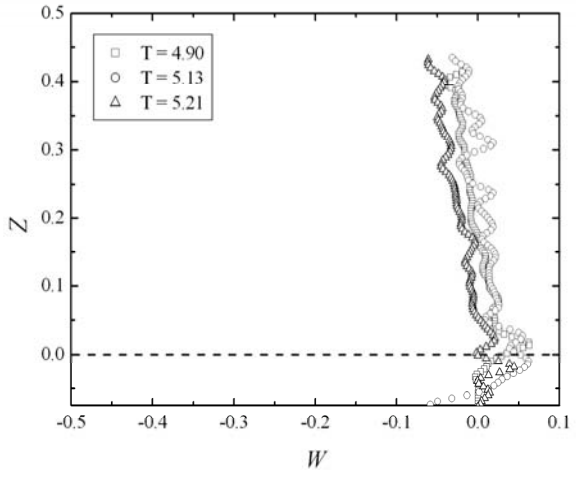

Figure 19. Profiles of vertical velocity for $T = 4.90$, 5.13 and 5.21 at $X = 0.5$.

When looking at the velocity field angle in Figure 20 it is possible to see how significantly the flow has changed since the first time instants. From Figure 20 it is clear that the velocity field is practically horizontal at $T = 4.90$.

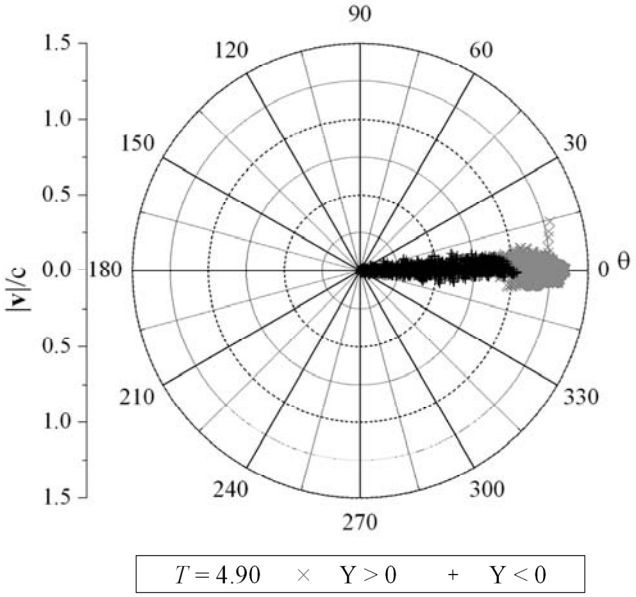

Figure 20. Velocity vector angle and modulus distribution for $T = 4.90$. Concentric circles represent a value of constant velocity, whose scale is represented by the vertical line adjacent to the plot.

4.2.1 *Detailed Analysis of the Sediment Layer*

A similar analysis to the one presented in 4.1.1 is made for the far field conditions.

For this case the velocity field is more regular than the one depicted in Figure 11 ($T = 0.44$). The vector field of the sediment layer and the vector field of the water layer have the same angle.

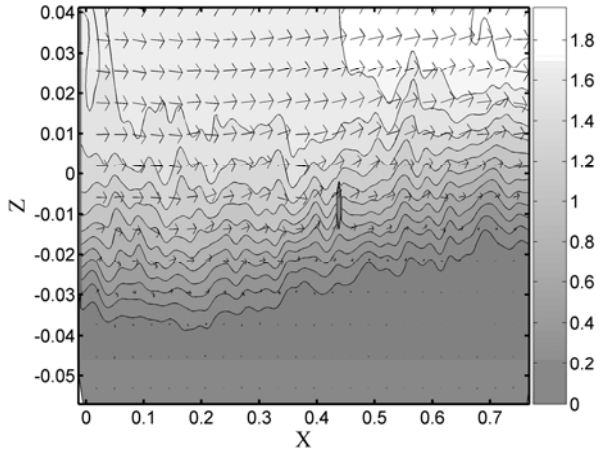

Figure 21. Detail for the velocity field near bed region for $T = 4.90$. For clarity only 1 out of 8 vectors are represented along the horizontal and 1 out of 2 is represented along the vertical.

5 CONCLUSIONS

The two-dimensional dam break flow over a moving bed of sediments was studied using Particle Image Velocimetry. This technique allowed the determination of the velocity field with a good spatial resolution (2 mm) and a time resolution of 0.067 s between pairs of images.

The flow can be divided in two typical behaviours depending on time and space: the near-field behaviour and the far-field behaviour. The results here presented for the near field time/space show the flow has a strong vertical component that in modulus is of the same order of magnitude as the horizontal component. As a direct consequence the velocity field has a severe downward inclination as depicted in Figure 10. For this case one may assume that $U \sim V$. The water layer velocity profiles at $X = 0$ suggest that there is a flow deceleration between $T = 0.67$ and $T = 0.77$ (Figure 8 and 9) before it accelerates again as shown for the far field case (Figure 16 and 17).

For the far field time/space the water layer presents a more uniform velocity profile, while the vertical component becomes practically zero. One can therefore say that $U >> V$. Measurements carried out for the hydrodynamic dam-break flow, i.e., without sediments, have shown a similar behaviour (Aleixo et al., 2009).

The sediment layer velocity field was also measured by using the sediments themselves as PIV seeding. As pointed out the results are biased by the detection of sediments out of the laser light sheet plane, but assuming that the sediment flow is only two-dimensional this effect can be neglected. Nevertheless a deeper analysis of the bias introduced by the sediments out of the laser light sheet plane should be carried out.

The results obtained show that the sediment horizontal velocity component is linearly distributed along the vertical, while the vertical component only shows such behaviour for the near field conditions. In the far field the vertical component of the sediment velocity field is practically zero.

ACKNOWLEDGMENTS

The present work was made possible by a PhD support for the first author under scholarship SFRH/BD/36023/2007 from the Fundação para a Ciência e Tecnologia, Portugal.

The PIV equipment used was funded by the Convention 2.4.526.08 du Fonds de la Recherche Fondamentale Collective (Fonds de la Recherche Scientifique), Belgium.

REFERENCES

Aleixo, R., Spinewine, B., Soares-Frazão, S., Zech Y. 2009. Non-intrusive measurements of water surface and velocity profiles in a dam-break flow. Proc. of the 33rd Inter. Assoc. of Hydraulic Eng. & Research (IAHR) Biennial Congress Vancouver, Canada, August 9-14.

Bailly, D., Van Reybroeck, A. 2003. Conception et réalisation d'un canal pour la modélisation expérimentale de la propagation sur lit mobile de l'onde de rupture d'un barrage. MSc. thesis, Université catholique de Louvain. Belgium.

Keane, R.D.., Adrian, R.J. 1992. Theory of Cross-correlation analysis of PIV images. Applied Scientific Research 49, 191-215

Lauber, G., Hager, W.H. 1998. Experiments to dambreak wave: horizontal channel. Journal of Hydraulic Research, 36, 291-307.

Raffel, M., Willert, C., Werely, S., Kompenhans, J. 2007. Particel Image Velocimetry – A practical guide 2nd Edition. Springer.

Soares-Frazão, S., Zech, Y. A. 2008. Dam-break flow through an idealised city. Journal of Hydraulic Research, 46(5), 648-658.

Spinewine B., Zech, Y., 2007. Small-scale laboratory dam-break waves on movable beds", Journal of Hydraulic Research Vol. 45 Extra Issue, pp. 73-86.

Spinewine B. 2005. Two-layer flow behaviour and the effects of granular dilatancy in dam-break induced sheet-flow. PhD thesis, Université catholique de Louvain, Belgium.

Stoker, J.J. 1957. Water waves: the mathematical theory with applications. Interscience. New York.

Van Goethem, J-L., Villers, L. 2000. Modélisation du transporte solide associé à l'onde de rupture d'un barrage : développement d'un schéma numérique aux voulmes finis et analyse de mesures expérimentales par techniques d'imagerie digitale. MSc. thesis, Université catholique de Louvain. Belgium.

Voisin, T., Greindl, A. 2007. Analyse expérimentale et théorique du profil vertical de vitesse: étude en écoulement permanent et en écoulement transitoire sévère MSc. thesis, Université catholique de Louvain. Belgium.

Zech, Y., Soares-Frazão, S., Spinewine, B., le Grelle, N. 2008. Dam-break induced sediment movement: Experimental approaches and numerical modeling. Journal of Hydraulic Research, IAHR, 46 (2), 176-190.